HHS Public Access

Author manuscript

Chem Commun (Camb). Author manuscript; available in PMC 2021 November 11.

Published in final edited form as:

Chem Commun (Camb). 2020 November 11; 56(87): 13409–13412. doi:10.1039/d0cc05030j.

Multiplexable fluorescence lifetime imaging (FLIM) probes for Abl and Src-family kinases

Sampreeti Jena[±,c], **Nur P. Damayanti**[±,a,d], **Jackie Tan**[c], **Erica D. Pratt**[c], **Joseph M. K. Irudayaraj**[*,a,e], **L. L. Parker**[*,b,c]

[a]*Previous affiliation:* Department of Biochemistry, Molecular Biology and Biophysics, Masonic Cancer Center, University of Minnesota, Minneapolis, 55455.

[b]*Previous affiliation:* Department of Agricultural and Biological Engineering, Purdue University Center for Cancer Research, Purdue University, West Lafayette, IN, 47907.

[c]*Current affiliation:* Department of Medicinal Chemistry and Molecular Pharmacology, College of Pharmacy, Purdue Center for Cancer Research, Purdue University, West Lafayette, IN, 47907.

[d]*Current affiliation:* Indiana University School of Medicine, Indianapolis, IN, 46202.

[e]*Current affiliation:* Department of Bioengineering, University of Illinois at Urbana-Champaign, Urbana, IL, 61801.

Abstract

Many commonly employed strategies to map kinase activities in live cells require expression of genetically encoded proteins (e.g. FRET sensors). In this work, we describe the development and preliminary application of a set of cell-penetrating, fluorophore labelled peptide substrates for fluorescence lifetime imaging (FLIM) of Abl and Src-family kinase activities. These probes do not rely on FRET pairs or genetically-encoded protein expression. We further demonstrate probe multiplexing and pixel-by-pixel quantification to estimate the relative proportion of modified probe, suggesting that this strategy will be useful for detailed mapping of single cell and subcellular dynamics of multiple kinases concurrently in live cells.

Protein kinases control many fundamental aspects of cell function, including the cell cycle, DNA repair, and response to exogenous stimuli. Despite the biological importance of their dynamics and subcellular localization, few tools exist for monitoring kinase activities in cells in real time. Genetically-encoded Förster resonance energy transfer (FRET) protein sensors can accomplish single cell, dynamic imaging[1], however these are difficult to multiplex since two fluorophores (often with relatively broad excitation and emission spectra) are required per sensor, so spectral overlap/bleed through between sensors becomes a significant problem.

[*]Co-corresponding authors: llparker@umn.edu, jirudaya@illinois.edu.
[±]These authors contributed equally to this work.

Electronic Supplementary Information (ESI) available: Includes detailed experimental and data analysis procedures, probe characterization data, and additional fluorescence images.

We previously reported that a Cy5 fluorophore labelled, cell-penetrating peptide substrate for Abl kinase exhibited longer fluorescence lifetime upon phosphorylation and apparent interaction of the phosphopeptide product with SH2 domains.[2] This novel strategy was capable of detecting Abl kinase activity and inhibition in live cells, however it was not clear if the approach would be applicable to other kinases. The approach was recently extended to monitor apparent Akt, VEGFR2 and FAK activation in a range of cell models using 5-FAM, a fluorescein-based fluorophore label[3–4]—however, 5-FAM is known to be environmentally sensitive, so it was still not clear whether other, non-environmentally sensitive fluorophores would behave similarly in these probes. In this current report, we demonstrate that this strategy can be applied to the Src family, to additional fluorophore scaffolds (DyLight 488, a non-environmentally-sensitive fluorescein-like scaffold, and DyLight 550, a cyanine/Cy3-like scaffold that is also environmentally stable), and multiplexed analysis via multi-color labelling and imaging. The proof of concept was thoroughly validated by testing of suitable negative and positive control probes. Time lapse imaging was employed to investigate activity of Abl and Src family kinases simultaneously after EGF stimulation and subsequent inactivation by an inhibitor, visualizing their differential subcellular activation patterns and selectivity against two inhibitors. We also present a formula and MATLAB script by which the lifetime data in each cell, or even each pixel, can be used to extract fractional contributions from “unphosphorylated” and “phosphorylated” probe populations, paving the way to more detailed mapping of kinase activity and phosphorylation dynamics within cell populations and throughout the interior of a live cell.

We started by exploring the generality of the fluorescence lifetime shift upon phosphorylation of the peptide probe, using DyLight 488 and DyLight 550. Two substrates were chosen: Abltide (Abl kinase substrate, as we used in previous work)[2] and SFAStide-A (a Src-family kinase substrate previously developed by the Parker laboratory)[5] and conjugated with TAT to create cell-penetrating probes. Peptides were synthesized with the sequences shown in Table 1, labelled on the central cysteine residue by maleimide chemistry, and purified by preparative HPLC (as previously described[2]). The corresponding phosphorylated and Y→F mutant probes were also synthesized as positive and negative controls, respectively. Cell uptake incubation time was determined by characterizing probe uptake via flow cytometry using Abltide-Y→F-TAT mutant probe, as the Y→F mutant is the least likely to have modification affect its uptake and/or localization and thus can serve as a baseline model for probe uptake (Supporting information Fig. S1A). Cell viability was also assessed via flow cytometry, to ensure that the peptides were not toxic to cells (Fig. S1B).

We used a well-characterized model, previously validated by Parsons *et al.* (1996) and Plattner *et al.* (2006) among several others, in which Abl and Src-family kinases are known to be activated downstream of epidermal growth factor receptor (EGFR) stimulation by EGF.[6–7] This requires serum starvation to suppress basal kinase and phosphatase activities (amongst other signalling activities). After EGF is added to serum starved cells, the signalling cascade results in Src-family and Abl kinase activation. We then used the dual Abl/Src-family inhibitor dasatinib to test inhibition of those kinases.[8–9]

All three variants of SFAStide probes including the wild type (SrcF), synthetically phosphorylated (pSrcF), and Y→F (FmSrcF) mutants were labelled with DyLight 488 (DL488). These probes were tested in MDA-MB-231 cells for phosphorylation- and kinase activity-dependence of a fluorescence lifetime shift (Fig. S2, top and Fig. S3). The cells were incubated in media containing the probes (10 μM) for 2 hours. Imaging was performed as described in the Methods section (as in our previous publication).[2] As seen in Figure S2, longer lifetimes were observed for the wild type probes upon EGF stimulation, which can be attributed to phosphorylation by the respective kinase. Upon treatment with inhibitor, the lifetime distributions reverted to lower values and resembled distributions prior to stimulation indicating dephosphorylation of the probes by endogenous phosphatases, without the corresponding rephosphorylation that would have continued to occur in the absence of kinase inhibitor. The Y→F mutants did not shift to longer lifetimes even with EGF stimulation, supporting the concept that phosphorylation of the probe is required to generate the longer lifetime signal. The pY positive controls showed longer lifetimes preceding stimulation, which was expected based on the known suppression of phosphatase as well as kinase activities under serum starvation conditions, [10–14] such that the pY positive control probe maintains its phosphorylation state during uptake and incubation prior to EGF stimulation. The pY positive controls continued to exhibit longer lifetimes post-EGF stimulation, indicating that the balance between phosphatase/kinase activities on the enriched population of pY probes was maintained (as expected under these conditions[6, 12, 15–16]). Inhibitor treatment did result in lower lifetimes observed, consistent with phosphatase activity on the synthetically phosphorylated material not being balanced by corresponding kinase activity (as we have previously described).[2]

Abltide probes[2] labelled with DyLight 488 (Fig. S5) (ABL-DL488) and DyLight 550 (ABL-DL550) (Fig. S2, bottom and Fig. S4) were similarly characterized. EGF stimulation was also used to activate the Abl kinase (as previously reported) [6, 17] followed by treatment with the Abl inhibitor imatinib. Their lifetime distributions showed the expected trends with activity stimulation and inhibition, indicating that regardless of the type of fluorophore (DyLight 488 or DyLight 550, or Cy5 as shown in our previous work[2]), all probes showed a phosphorylation dependent lifetime shift, despite intrinsically different lifetimes of the fluorophores.

As a preliminary application of the Abl and Src-family probes in multiplexed analysis of kinase activation and inhibition, we performed experiments to monitor the difference between the effects of dasatinib vs. imatinib on Abl and Src-family kinase activation in EGF-stimulated MDA-MB-231 cells (Fig. 1 and Fig. S6). For this purpose, we used SrcF-DL488 and ABL-DL550. Serum-starved cells were incubated in a 50:50 mixture of the two probes (10 μM each) followed by activation of both Src and Abl via EGF stimulation, and subsequent treatment with dasatinib or imatinib. Multiplexed imaging was performed by sequential scanning with the respective excitation/emission channels for the two fluorophores, and lifetime information from the SrcF-DL488 and ABL-DL550 probes was extracted using the two detection channels per image. A threshold filter was applied to analyse only pixels with photon counts of at least 100 for the biexponential fit analysis. As a result, signal for each channel was not always equivalent (Fig. 1), giving rise to a punctate like appearance for the probe in some representative examples (Fig. S7)—however, this

intensity heterogeneity betweens did not affect consistency of lifetime distributions observed between replicates (highlighting the advantages of using lifetime as probe read-out rather than intensity). Both probes exhibited longer lifetime upon EGF stimulation that was subsequently decreased by dasatinib (which inhibits Src family kinases and Abl). In contrast, if the cells were treated with imatinib (which only inhibits Abl, but not Src family kinases), only the ABL-DL550 probe show decreased lifetime while lifetime distribution of the SrcF-DL488 probe remains virtually unchanged (Fig. 1). These results show that the FLIM probes can be efficiently multiplexed by tagging with fluorophores of different colours characterized by distinct excitation wavelengths and emission bandwidths. They also support the kinase activity dependence of the lifetime shift, and demonstrate the utility of this approach for measuring kinase inhibitor selectivity in live cells.

Next, to understand the dynamics of phosphorylation of the probes by the respective kinases, the ABL-DL488 probe was imaged over a time course following stimulation with EGF and subsequent treatment with imatinib (Fig. 2 and Fig. S9). As a surrogate for relative changes in phosphorylated probe, we sought to quantify the relative amount of the longer lifetime species. We used a multi-exponential fitting model to extract the proportion of the longer vs. shorter lifetime species on a per-image basis from the time course experiments. This was done by fitting the averaged decay curve for each image to a bi-exponential model function, employing the Levenberg–Marquardt routine for non-linear least squares fitting,[18] as further described in the Supporting Information. This fitting algorithm resolved two different lifetimes, as well as their fraction, to identify the average lifetime for each species. The relative intensity represented by the longer vs. the shorter lifetime species was then calculated and expressed as F_{long} (I_{long}/I_{total}). To extract the fraction of the longer lifetime component for individual pixels, a similar fitting analysis was performed on all pixels, iteratively, and the respective I_{long}/I_{total} corresponding to each pixel was spatially mapped. The fraction of the longer lifetime species was mapped on a pixel by pixel basis in the representative FLIM images. The overall fraction of the longer lifetime component (averaged across all pixels) is plotted as at 5 min intervals (Fig. 2). The longer lifetime component (phosphorylated population) progressively increased following EGF treatment and reached steady state after ~40 minutes, then declined following imatinib treatment, stabilizing at a proportion similar to that at the beginning of the stimulation by ~30–40 minutes. Following 3–4 rounds of imaging over the time course, a gradual decrease in overall emission intensity was observed, due to photobleaching of the fluorophores (e.g. Fig. S8), however this did not affect lifetime measurements—again highlighting the advantages of lifetime as a read-out, especially for time-course experiments.

Multiplexed time-course imaging was also performed, using Pulsed Interleaved Excitation (PIE), in which the system alternated between the two lasers (485 nm and 560 nm) and their respective detection channels in order to avoid excitation bleed through between the two fluorophores. The serum-starved MDA-MB-231 cells were incubated in a 50:50 mixture of SrcF-DL488 and Abl-DL550 (10 μM each), excess probe was removed and replaced with fresh serum-free colourless media, and the cells were imaged at 5 min intervals after treating with EGF (40 min) and dasatinib (an additional 40 min). The green and red channels were separately analysed to obtain lifetime information corresponding to SrcF-DL488 (Fig. 3A) and ABL-DL550 (Fig. 3B), respectively. As expected, F_{long} for both probes increased over

time after EGF stimulation and decreased after adding dasatinib. These analyses illustrate the potential to obtain subcellular maps of FLIM probe phosphorylation that could ultimately be used for more refined quantification of kinase activities in specific areas of the cell, paving the way towards incorporation of FLIM probe data into complex models of signalling behaviour both between and within individual cells.

Conclusions

In this work, we showed that combining different fluorophores and peptides into Abl and Src-family kinase FLIM probes exhibited similar phosphorylation-dependent lifetime behaviour, implying that the effects of phosphorylation via kinase activity on fluorescence lifetime of these probes are likely to be broadly applicable. Notably, fluorophores of very different molecular structures (an environmentally-stable fluorescein-like dye and two different cyanine dyes) resulted in the same lifetime shift trends upon probe phosphorylation. Our previous work only used the cyanine dye Cy5, which contains two quaternary nitrogen-containing heteroaromatic rings (which hold permanent positive charge) connected by a conjugated alkene linker, and it was reasonable to suppose that interaction between that particular structure and the SH2 domain may have contributed to the lifetime change. The fluorescein-like scaffold, in contrast, is comprised of a polyaromatic heterocyclic structure with no nitrogens, and with substantial negative charge at physiological pH. By showing that the fluorescein-type scaffold (DyLight-488) and the shorter Cy3-like scaffold (DyLight-550) both result in a lifetime shift, we substantially expand the potential scope for this strategy, since it appears that the effect is fluorophore-agnostic. Further characterization of the interaction between these peptide probes and SH2 domains is underway. We also demonstrated for these FLIM probes that the relative proportions of the individual lifetime sub-populations can be quantified via multicomponent fitting on a pixel-by-pixel basis to infer relative changes in probe phosphorylation. It is important to note that this is not a measure of % phosphorylation or phosphorylation rate by the kinase, however the relative rates of change in proportion between the lifetime species can at least serve as a surrogate to assess alterations in relative kinase activity under different conditions. These results show the generality and multiplexability of this approach to quantify proportions of phosphorylated and unphosphorylated species and provide a specific strategy for more advanced quantitative study of subcellular kinase activity trends using these and similar probes.

Supplementary Material

Refer to Web version on PubMed Central for supplementary material.

‡ Acknowledgements:

Cells used in this work were a kind gift from Prof. Robert Geahlen (Purdue University Department of Medicinal Chemistry and Molecular Pharmacology). This work was supported by the Purdue Center for Cancer Research (NPD and JI) and the NCI/NIH (R01CA182543 and R33CA217780 to LLP).

Notes and references

1. Lin W; Mehta S; Zhang J, Genetically encoded fluorescent biosensors illuminate kinase signaling in cancer. Journal of Biological Chemistry 2019, 294 (40), 14814–14822. [PubMed: 31434714]
2. Damayanti NP; Parker LL; Irudayaraj JM, Fluorescence lifetime imaging of biosensor peptide phosphorylation in single live cells. Angew Chem Int Ed Engl 2013, 52 (14), 3931–4. [PubMed: 23450802]
3. Damayanti NP; Buno K; Cui Y; Voytik-Harbin SL; Pili R; Freeman J; Irudayaraj JMK, Real-Time Multiplex Kinase Phosphorylation Sensors in Living Cells. ACS Sens 2017, 2 (8), 1225–1230. [PubMed: 28838242]
4. Damayanti NP; Buno K; Narayanan N; Voytik Harbin SL; Deng M; Irudayaraj JMK, Monitoring focal adhesion kinase phosphorylation dynamics in live cells. Analyst 2017, 142 (15), 2713–2716. [PubMed: 28589989]
5. Lipchik AM; Perez M; Bolton S; Dumrongprechachan V; Ouellette SB; Cui W; Parker LL, KINATEST-ID: A Pipeline To Develop Phosphorylation-Dependent Terbium Sensitizing Kinase Assays. J Am Chem Soc 2015, 137 (7), 2484–94. [PubMed: 25689372]
6. Srinivasan D; Plattner R, Activation of Abl tyrosine kinases promotes invasion of aggressive breast cancer cells. Cancer research 2006, 66 (11), 5648–5655. [PubMed: 16740702]
7. Biscardi JS; Belsches AP; Parsons SJ, Characterization of human epidermal growth factor receptor and c-Src interactions in human breast tumor cells. Molecular Carcinogenes is: Published in cooperation with the University of Texas MD Anderson Cancer Center 1998, 21 (4), 261–272.
8. Rix U; Hantschel O; Dürnberger G; Remsing Rix LL; Planyavsky M; Fernbach NV; Kaupe I; Bennett KL; Valent P; Colinge J, Chemical proteomic profiles of the BCR-ABL inhibitors imatinib, nilotinib, and dasatinib reveal novel kinase and nonkinase targets. Blood, The Journal of the American Society of Hematology 2007, 110 (12), 4055–4063.
9. Montero JC; Seoane S; Ocaña A; Pandiella A, Inhibition of SRC family kinases and receptor tyrosine kinases by dasatinib: possible combinations in solid tumors. Clinical cancer research 2011, 17 (17), 5546–5552. [PubMed: 21670084]
10. Pirkmajer S; Chibalin AV, Serum starvation: caveat emptor. American Journal of Physiology-Cell Physiology 2011, 301 (2), C272–C279. [PubMed: 21613612]
11. Mandl A; Sarkes D; Carricaburu V; Jung V; Rameh L, Serum withdrawal-induced accumulation of phosphoinositide 3-kinase lipids in differentiating 3T3-L6 myoblasts: distinct roles for Ship2 and PTEN. Molecular and cellular biology 2007, 27 (23), 8098–8112. [PubMed: 17893321]
12. Zhao Z; Tan Z; Diltz CD; You M; Fischer EH, Activation of mitogen-activated protein (MAP) kinase pathway by pervanadate, a potent inhibitor of tyrosine phosphatases. Journal of Biological Chemistry 1996, 271 (36), 22251–22255. [PubMed: 8703041]
13. Sarhan AR; Patel TR; Cowell AR; Tomlinson MG; Hellberg C; Heath JK; Cunningham DL; Hotchin NA, LAR protein tyrosine phosphatase regulates focal adhesions through CDK1. J Cell Sci 2016, 129 (15), 2962–2971. [PubMed: 27352860]
14. Galic S; Klingler-Hoffmann M; Fodero-Tavoletti MT; Puryer MA; Meng T-C; Tonks NK; Tiganis T, Regulation of insulin receptor signaling by the protein tyrosine phosphatase TCPTP. Molecular and cellular biology 2003, 23 (6), 2096–2108. [PubMed: 12612081]
15. Irwin ME; Bohin N; Boerner JL, Src family kinases mediate epidermal growth factor receptor signaling from lipid rafts in breast cancer cells. Cancer biology & therapy 2011, 12 (8), 718–726. [PubMed: 21775822]
16. Reddy RJ; Gajadhar AS; Swenson EJ; Rothenberg DA; Curran TG; White FM, Early signaling dynamics of the epidermal growth factor receptor. Proceedings of the National Academy of Sciences 2016, 113 (11), 3114–3119.
17. Ganguly SS; Plattner R, Activation of abl family kinases in solid tumors. Genes & cancer 2012, 3 (5–6), 414–425. [PubMed: 23226579]
18. Levenberg K, A method for the solution of certain problems in least squares. Q Appl Math 2: 164–168 Marquardt D (1963) An algorithm for least-squares estimation of nonlinear parameters. SIAM J Appl Math 1944, 11 (2), 431–441.

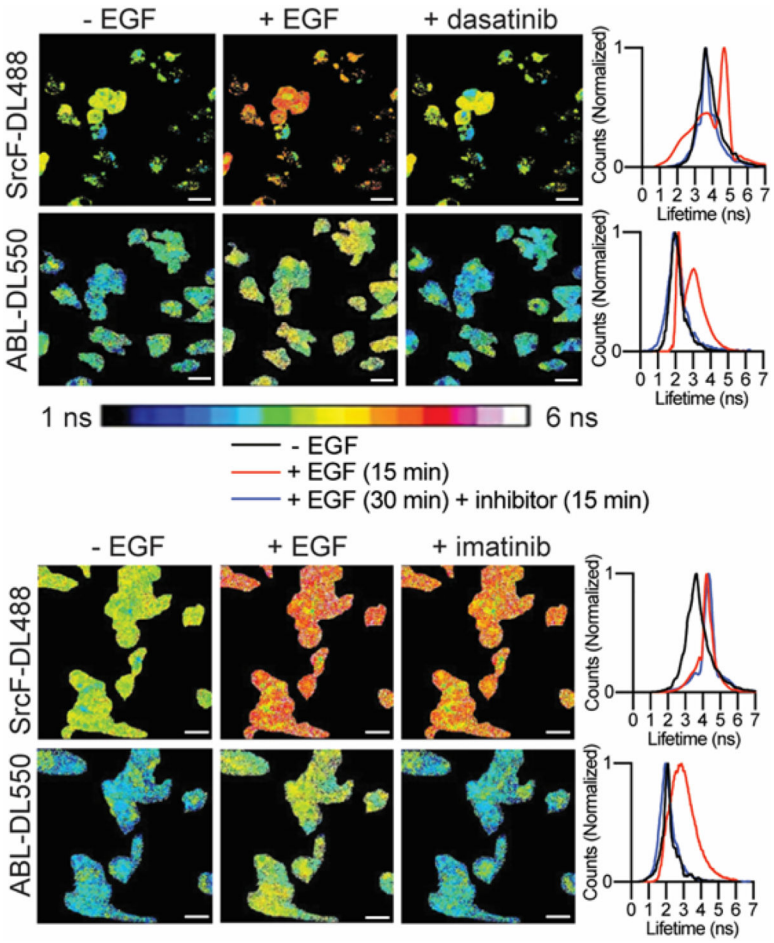

Figure 1: Dasatinib inhibits phosphorylation of both ABLtide and SFAStide probes (Top). Imatinib inhibits phosphorylation of ABLtide probe but not the SFAStide probe (Bottom).

ABL-DL550 and SrcF-DL488 probes (10 μM each) were incubated with serum-starved MDA-MB-231 cells for 2 h. Kinase activity was stimulated with EGF (10 ng) for 15 min, followed by addition of inhibitor imatinib or dasatinib (1 μM) for an additional 15 min. Images normalized to the lifetime scale and average lifetime histograms corresponding to the green (top row) and red (bottom row) channels are shown. Scale bars are 20 μm.

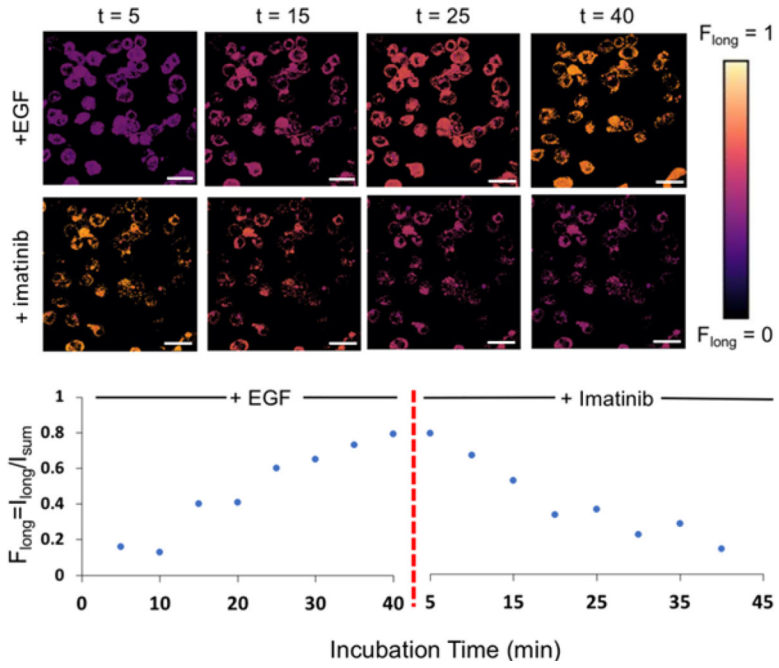

Figure 2: Quantitation of relative probe phosphorylation.

FLIM data from time course experiments with ABL-DL488 probe were analysed via bi-exponential fitting as described in the supporting information, quantifying relative amount of phosphorylated probe per pixel following EGF treatment (top row) and subsequent imatinib treatment (bottom row). The relative fraction of phosphorylated probes (F_{long}) is plotted as quantitative subcellular maps. The F_{long} value averaged over all the pixels is also plotted as a function of time. Scale bars are 20 μm.

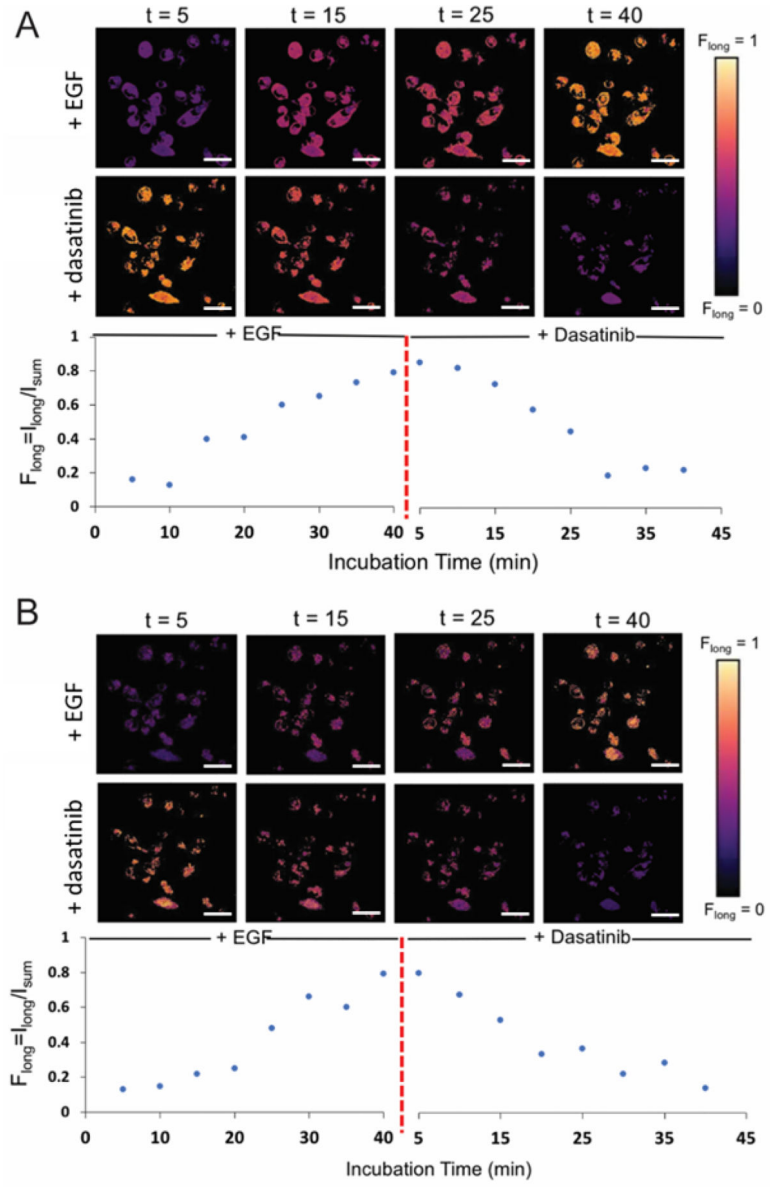

Figure 3: Quantitation of relative probe phosphorylation in multiplexed probes.

FLIM data from EGF stimulation and dasatinib inhibition experiments of (A) SrcF-DL488 and (B) ABL-DL550 probes were analysed via bi-exponential fitting to quantify the relative amount of phosphorylated probe per pixel, following EGF treatment (top row) and imatinib treatment (bottom row).

Table 1.

Peptide probe sequences

Probe	Sequence
SFAStide-A-TAT	GG**DEDIYEELD**C̲GG*RKKRRQRRRPQ*
pSFAStide-A-TAT	GG**DEDIpYEELD**C̲GG*RKKRRQRRRPQ*
SFAStide- A-Y→F-TAT	GG**DEDIFEELD**C̲GG*RKKRRQRRRPQ*
Abltide-TAT	GG**EAIYAAP**C̲GG*RKKRRQRRRPQ*
pAbltide-TAT	GG**EAIpYAAP**C̲GG*RKKRRQRRRPQ*
Abltide-Y→F-TAT	GG**EAIFAAP**C̲GG*RKKRRQRRRPQ*

Sequences in **bold** are the substrate portion; in *italic* is the TAT cell-penetrating module; C̲ = the cysteine used for fluorophore labelling; pY = phosphorylated tyrosine.